THERMOELECTRIC MICROSTRUCTURES OF BI_2TE_3 / SB_2TE_3 FOR A SELF-CALIBRATED MICROPYROMETER

L. M. Goncalves(1)*, C. Couto(1), P. Alpuim(2), D. M. Rowe(3), J. H. Correia(1)
(1) Department of Electronics, University of Minho, Portugal
(2) Department of Physics, University of Minho, Portugal
(3) School of Engineering, University of Cardiff, UK
* e-mail: lgoncalves@dei.uminho.pt

ABSTRACT

The fabrication (using planar thin-film technology) of Bi_2Te_3 and Sb_2Te_3 microstructures, with high thermoelectric figure of merit, suitable for incorporation in Peltier elements and thermopiles, is reported. The microstructures were fabricated by co-evaporation of Bi and Te, for the n-type element, and Sb and Te, for the p-type element, on a 25 μm-thick polyimide (kapton) substrate. Kapton film is a flexible, robust substrate with a low thermal conductivity. While the plastic mechanical properties allow conformal coverage of surfaces with many different shapes without apparent damage of film or substrate, Kapton low conductivity ensures that the devices will not be thermally shorted through the substrate. High figures of merit are reported, sufficient to achieve more than 10ºC of cooling over a 1 mm^2 area.

Keywords: thermoelectric, thin-film, pyrometer, Peltier, micro-cooler.

INTRODUCTION

Local cooling of electronic micro devices has become an area of increasing interest in recent years. Thermoelectric cooling is an advantageous choice for cooling, since it does not imply the use of mechanical moving parts, can be integrated in microelectronic circuits and is easily controlled. Thermoelectric devices may also have the capability of reverse operation: they can be used as electrical generators, converting thermal energy in electric energy. The thermoelectric performance of the devices is characterized by the dimensionless figure of merit parameter (ZT):

$$ZT = \frac{\alpha^2}{\rho\lambda} T \qquad (1)$$

where α is the Seebeck coefficient, ρ the electrical resistivity, λ the thermal conductivity and T the temperature [1].

Although there is no physical limit for the value of ZT, thermoelectric materials did not exceed ZT~1 for almost 50 years. In the last few years, a significant improvement in materials properties has been reported. Venkatasubramanian et al. [2] reports a figure of merit of 2.4, with ultra-thin layers of two alternating semiconductors.

While the search for thermoelectric materials with high figure of merit continues, efforts are currently made to achieve compatibility with solid-state electronic materials. Tellurium alloys (Bi_2Te_3 and Sb_2Te_3) are well-established low-temperature thermoelectric materials and are widely employed in thermoelectric generators and coolers [1]. In the present work, planar thin film technology will be used to fabricate such devices.

Different deposition techniques can be used to deposit Bi-Sb-Te thin films. Thermal co-evaporation [3], co-sputtering [4], electrochemical deposition [5], metal-organic chemical vapour deposition [6] and flash evaporation [7] are some examples.

Two different approaches can be used to on-chip integration of thermoelectric coolers: transversal (cross-plane) and lateral (in-plane), depending on the direction in which de energy is removed, relative to the surface of the device. In this work, lateral cooling is addressed, due to its easier fabrication process and compliance with planar technology.

In this paper, Bi_2Te_3 and Sb_2Te_3 are used to fabricate a Peltier thermoelectric cooler and a radiation detector (bolometer) based on a thermopile in a standing bridge (figure 4). Using the cooler to stabilize the cold side of the bolometer at a given temperature, allows the self-calibrating method described [8] to be achieved on a single chip.

THERMOELECTRIC FILMS

Tentative deposition of Bi_2Te_3 and Sb_2Te_3 films by direct evaporation of the compounds proved to be not appropriate due to the large differences in vapour pressures of bismuth or antimony and tellurium, resulting in a compositional gradient along the film thickness. This result was also reported in the literature [9].

The thermoelectric films were fabricated by co-evaporation [3] of Bi and Te, for the n-type element (Bi_2Te_3), and of Sb and Te, for the p-type element (Sb_2Te_3), on a 25 μm-thick flexible kapton substrate.

Plastic film was chosen as substrate for being flexible, robust and having low-thermal conductivity. While plastic mechanical properties are advantageous for integration with any type of flexible electronic device, the choice for kapton was due to its low thermal conductivity of 0.12 $Wm^{-1}K^{-1}$, and its value of thermal expansion coefficient (12×10^{-6} K^{-1}) which closely matches the thermal expansion coefficient of the films, thus reducing residual stress and increasing adhesion. The co-evaporation method is inexpensive, simple, and reliable, when compared to other techniques that need long time periods to prepare the starting material or require more complicated and expensive deposition equipment. During deposition the substrate was heated to temperatures in the range 200ºC-300ºC. Two crystal oscillators and thickness monitors were used to monitor the deposition rate of Bi/Sb and Te. Each rate was maintained at a fixed value, through control of the power applied to each molybdenum evaporation boat.

Table1. Deposition parameters

Film	*Substrate Temperature*	*Evaporation rate (Bi or Sb)*	*Evaporation rate (Te)*
Bi_2Te_3	270 ºC	1 Aº/sec	2.2 Aº/sec
Sb_2Te_3	230 ºC	1 Aº/sec	2.2 Aº/sec

A computed PID controller was implemented to compute and adjust in real time the power applied to the evaporation boats and thus achieve constant evaporation rates. Table 1 shows the optimized deposition parameters used in fabrication of n-type and p-type films.

Table2. Stoichiometry of films obtained by EDX

Film	*%Te*	*%Bi or %Sb*
Bi_2Te_3	60.17%	39.83%
Sb_2Te_3	58.51%	41.49%

Energy-dispersive X-ray spectroscopy shows the composition of the best n-type and p-type films (table 2).

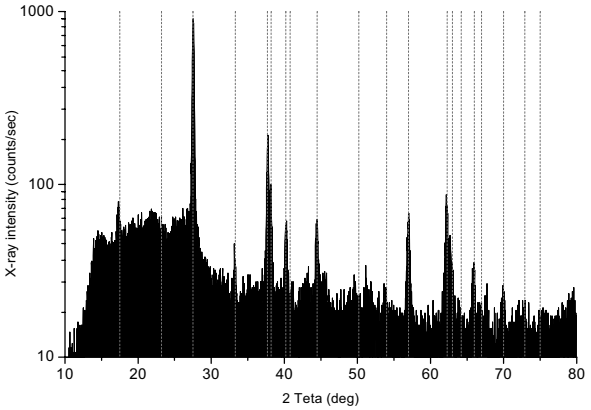

Figure 1. XRD analysis of an n-type Bi_2Te3 thin film. The peaks agree with the powder diffraction spectrum for Bi_2Te_3 (dashed lines).

Te and Bi (Sb) content shows that the composition of both types of films is close to stoicheometry. X-ray diffraction analysis reveals the polycrystalline structure. The peaks agree with the powder diffraction spectrum for polycrystalline Bi_2Te_3 and Sb_2Te_3 [Figures 1 and 2].

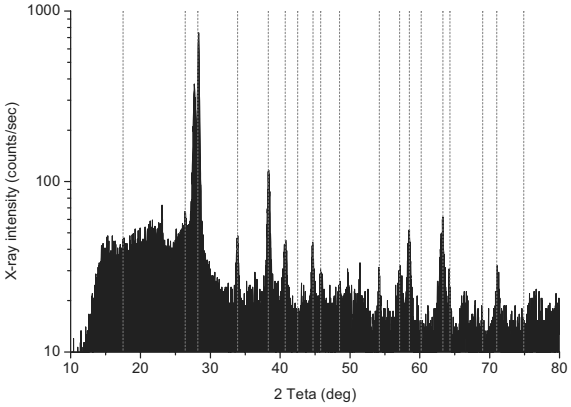

Figure 2. XRD analysis of a p-type Sb_2Te_3 thin film. The peaks agree with the powder diffraction spectrum for Sb_2Te_3 (dashed lines).

In-plane film electrical resistance was measured using conventional four probe van der Pauw method, at room temperature. Seebeck coefficient was measured by connecting one side of the film to a fixed temperature (heated metal block) and the other side to a heat sink at room temperature. Table 3 shows the results of these measurements and the corresponding figure of merit at 300 K (thermal conductivity of 1.5 $Wm^{-1}K^{-1}$ assumed for calculations).

Table3. Thermoelectric properties of films in the present work.

Film	*Seebeck*	*Resistivity*	*Figure of merit*
Bi_2Te_3	-189 µV/ºC	7.7 µΩm	0.93
Sb_2Te_3	140 µV/ºC	15.1 µΩm	0.26

Bi_2Te_3 films exceeded performance of bulk material, reported in literature. Sb_2Te_3 films could not attain the same high-level of performance. The values in table 3 are higher than reported for films deposited by co-sputtering or electrochemical deposition, and are close to those

Table4. Thermoelectric properties of p and n-type films from the literature.

Film	*Method*	*Seebeck*	*Resistivity*	*Figure of*
		µV/ºC	*µΩm*	*merit*
Bi_2Te_3	Co-Sput. [4]	-160	16.3	0.31
Bi_2Te_3	MOCVD [6]	-210	9.0	0.98
Bi_2Te_3	Co-Evap. [3]	-228	13	0.80
Bi_2Te_3	ECD. [5]	-60	10	0.07
Bi_2Te_3 *	Flash [7]	-200	15	0.53
Sb_2Te_3	MOCVD [6]	110	3.5	0.69
Sb_2Te_3	Co-Evap. [3]	171	10.4	0.56

reported for films deposited by metalorganic chemical vapour deposition or flash evaporation (table 4). Thermal conductivity of 1.5 $Wm^{-1}K^{-1}$ is assumed on all authors.

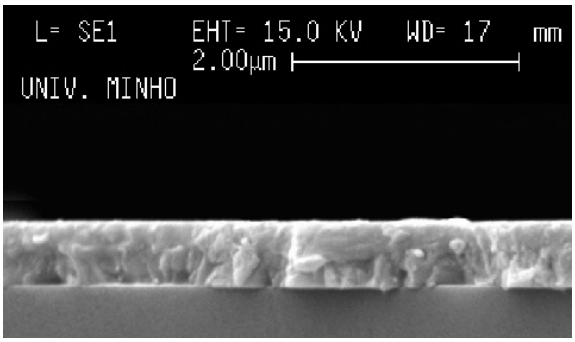

Figure 3: A SEM photo of a homogeneous n-type 580 nm-thick Bi_2Te_3 film deposited onto a glass substrate.

DEVICE SIMULATION

A Peltier cooler and a thermopile, based on the n-type and p-type materials described above, are under construction on a free standing silicon nitride bridge [Figure 4] obtained by anisotropic etching of bulk silicon from the back of the wafer.

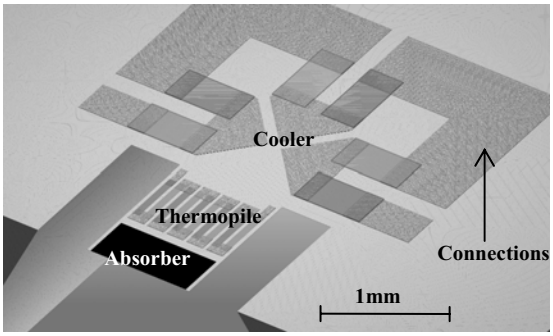

Figure 4. The micropyrometer is composed of Peltier cooler, thermopiles and a black gold strip absorber.

The thermopile will be used in a bolometer structure, to measure the temperature rise caused by radiation absorbed in the absorber, a black gold strip build on the silicon nitride membrane. The Peltier cooler is used to stabilize the temperature of the bolometer at specific values. Finite element analysis, considering radiation and convection losses, shows the possibility to obtain a 10 K cooling of the bolometer assuming a 650 μWmm^{-2} thermal power absorbance in the absorber of the radiation sensor [Figure 6]. The thermal power absorbed by the radiation sensor is given by:

$$Q_{RAD} = \varepsilon.\sigma.\left(T_O^4 - T_S^4\right).A_S \qquad (2)$$

ε is the emissivity of the sensor, T_O the object temperature, T_S the sensor temperature and A_S the absorber area. The top part of the absorber receives radiation from an hypothetical distant object being measured and the bottom part radiates to substrate temperature. When convection to air is considered the following approximation can be used:

$$Q_{conv} = 0.61\left(\frac{\Delta T}{L}\right)^{0.2} A_S.\Delta T \qquad (3)$$

ΔT is the temperature difference between sensor and air and L the size of the sensor. Each PN pair of the peltier cooler can be modelled [10] by the following equation:

$$\Delta T = \frac{1}{K_e}(\alpha_p - \alpha_n)T_c I - \frac{1}{2}R_e I^2 - Q_{\mathrm{LOAD}} \qquad (4)$$

ΔT is the maximum temperature difference achieved by the cooler, α_p and α_n are the Seebeck coefficients of the p and n-type materials, respectively, T_c is the cold side temperature, I is the current applied and Q_{LOAD} is the sum of all thermal loads applied. R_e and K_e are the equivalent electrical resistance and thermal conductance of n and p elements and include the effects of substrate and contact resistances.

$$R_{eq} = \rho_n \frac{L_n}{W_n H_n} + \rho_p \frac{L_p}{W_p H_p} + 2\left(\frac{\rho_{cn}}{L_c W_n} + \frac{\rho_{cp}}{L_c W_p}\right) \qquad (5)$$

$$K_{eq} = \lambda_n \frac{W_n H_n}{L_n} + \lambda_p \frac{W_p H_p}{L_p} + \lambda_m \frac{W_m H_m}{L_m} \qquad (6)$$

Equation 4 assumes that the hot side of the cooler is connected to a highly thermal conductive material and to a heat sink, capable of keeping the hot side of the device at room temperature. This could be achieved in the model, with a silicon substrate.

The thermal circuit of the cooler can be modelled with an electrical spice simulator, using schematic on figure 5.

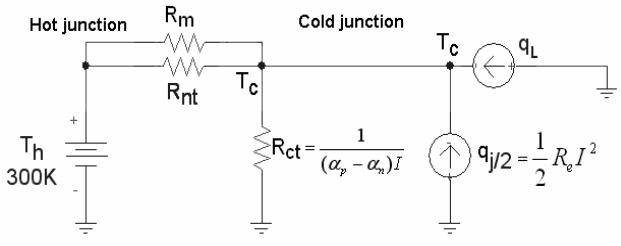

Figure 5. Schematic model of a Peltier cooler

R_m and R_{nt} are membrane and thermoelectric element thermal resistances, respectively. R_{ct} represents the heat removed by Peltier effect. The model is valid if the heat

sink in the hot junction can maintain this junction at 300K, as assumed before.

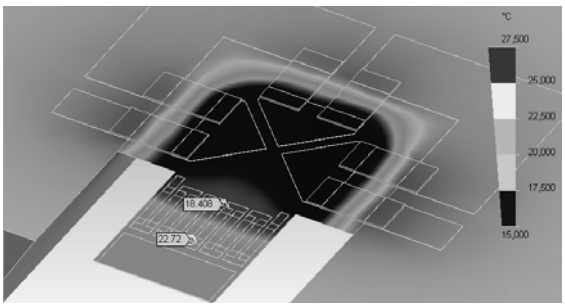

Figure 6. Finite element analysis shows the possibility to obtain 10 K cooling of the bolometer.

SELF-CALIBRATED PYROMETER

In a pyrometer, the radiation absorbed depends on the difference between the (unknown) temperature and emissivity of the target object and the temperature and emissivity of the absorber in the bolometer. It is impossible to compute the temperature of the target without calibrating the pyrometer with target object emissivity. In order to realize the self calibration method announced [8], an array of micropyrometers will be tuned for different radiation wavelengths, with several different temperatures of the bolometers set by the Peltier devices. The Peltier cooler has a small time constant because of the reduced dimensions, making it possible to set different temperatures of the bolometer during a temperature reading process, according to self-calibration method described [8].

$$U_1 = K.\sigma\left(T^4 - T_{s1}^4\right) \qquad U_2 = K.\sigma\left(T^4 - T_{s2}^4\right)$$

$$T = \sqrt[4]{\frac{U_1.T_{s2}^4 - U_2.T_{s1}^4}{U_1 - U_2}}$$

σ - Emissivity K – Sensor constants

T – Target temperature T_{sn} – nth sensor temperature

Figure 6. Equations to compute the target temperature, using the values obtained by two micropyrometers cooled to different temperatures [8].

Industrial application of a network of micropyrometers for measuring the temperature of textiles in movement, operating in the 20-100 ºC measuring range, representing a bandwidth of 5-20 μm in wavelength, is the final goal of this work.

CONCLUSION AND FUTURE WORK

A simple and inexpensive method to produce state-of-the-art Bi_2Te_3 and Sb_2Te_3 materials in the form of thin films was applied. Co-evaporation allows deposition of good thermoelectric materials, with a large figure of merit. The effect of evaporation rate of materials and substrate temperature in the fabrication of thermoelectric films was studied and optimized. Calculations and FEM simulations showed the potential to achieve more than a 10ºC cooling of the thermopile detector.

Kapton polyimide was used as the flexible substrate, for its low thermal conductivity. Thin silicon nitride standing bridges with low thermal conductivity, fabricated by back-side wet etching will allow reducing the dimensions of the bolometer and achieving faster cooling. The use of silicon also opens the possibility for integration of the electronics, the radiation sensor and the cooler on the same silicon chip, making it possible to produce a self-calibrated pyrometer on a single chip.

REFERENCES

[1] D.M. Rowe, “CRC Handbook of Thermoelectrics,” CRC Press, (1995).

[2] R. Venkatasubramanian, E. Siivola, T. Colpitts, and B. O’Quinn, “Thin-film thermoelectric devices with high room-temperature figures of merit,” Nature, vol. 413, 6856, 597, (2001).

[3] Helin Zou, D.M. Rowe, S.G.K. Williams, “Peltier effect in a co-evaporated Sb_2Te_3(P)-Bi_2Te_3(N) thin film thermocouple,” Thin Solid Films, 408, 270, (2002)

[4] Harald Böttner et al, “New Thermoelectric Components Using Microsystem Technologies,” Journal of Microelectromechanical Systems, 3, 414, (2004)

[5] J.R. Lim, G.J. Snyder, C.K. Huang, J.A. Herman, MA. Ryanand, J.P. Fleurial, “Thermoelectric Microdevice Fabrication Process and Evaluation at the Jet Propulsion Laboratory,” ICT2002

[6] A Giani et al., “Growth of Bi_2Te_3 and Sb_2Te_3 thin films by MOCVD,” Materials Science and Engineering, B64, 19–24, (1999)

[7] A. Foucaran, “Flash evaporated layers of (Bi_2Te_3–Bi_2Se_3)(N) and (Bi_2Te_3–Sb_2Te_3)(P),” Materials Science and Engineering, B52, 154–161, (1998)

[8] Lubos Hes, C. Couto, “Method of contactless measuring the surface temperature and/or emissivity of objects,” Patent 0 623 811 A1, (1994)

[9] Luciana W. da Silva and Massoud Kaviany, “Miniaturized Thermoelectric Cooler,” IMECE’02

[10] Gao Min, D.M. Rowe, “Cooling performance of integrated thermoelectric Microcooler,” Solid-State Electronics, 43, 923-929, (1999)